

# High-Symmetry Coordination Cages via Self-Assembly

S. RUSSELL SEIDEL\* AND PETER J. STANG\*

Department of Chemistry, University of Utah,  
315 South 1400 East, Room 2020, Salt Lake City, Utah 84112

Received May 14, 2002

## ABSTRACT

We provide a summary of our results in three-dimensional, coordination-driven self-assembly based on the directional-bonding methodology, in which the stoichiometric mixing of complementary building blocks, with appropriate, predefined geometries, leads to targeted, nanoscopic cages. Using this motif, we have synthesized high-symmetry ensembles resembling the Platonic solids, such as dodecahedra, and the Archimedean solids, such as truncated tetrahedra and cuboctahedra, as well as other cages, like trigonal bipyramids, adamantanoids, and trigonal prisms. The synthesis and characterization of these compounds is discussed, as is some host–guest chemistry.

## Introduction

Over the past few billion years, nature has crafted a design strategy, that of self-assembly, which is simultaneously elegant in both its simplicity and its complexity. This apparent paradox can be explained when viewing the different levels in the hierarchy of biological design. At the base level are the subunits, or building blocks, which are relatively simple in their composition and interactions that serve to bind them one to another. Yet, at the top levels, when the subunits are combined into their higher order structures, the results are stunning in their structural intricacy and sheer size, their functionality and selectivity, and their cooperation among themselves within living organisms. Self-assembly in nature is often based on numerous hydrogen-bonding, van der Waals, and many other weak inter-/intramolecular interactions working synergistically, and examples where it plays a key role abound.<sup>1,2</sup> For instance, the polymerization of actin monomers into filaments, which are most likely vital to the various functions of the cytoplasm of cells, such as cell shape and organelle movement, proceeds via self-assembly.<sup>3</sup> Likewise, the viral coats of all viruses are the product of nature's self-assembly processes.<sup>2</sup> These are

but two instances of self-assembly in a wide array of examples that permeates throughout known biological systems.

Nature has also intrigued and inspired man for millennia with its symmetry and beauty. Many of the ancient Greek mathematicians, such as Plato and Euclid, investigated the Platonic solids (Chart 1).<sup>4</sup> This set of five convex polyhedra comprises the tetrahedron ( $T_d$  symmetry), the cube and octahedron ( $O_h$  symmetry), and the dodecahedron and icosahedron ( $I_h$  symmetry).<sup>5</sup> Separating these solids from others is their high symmetry and the fact that all of them have faces consisting of only a single regular polygon (i.e., pentagonal faces for the dodecahedron). Another class of high-symmetry, convex polyhedra is the Archimedean solids, whose faces consist of two or more regular polygons (Chart 2). The roots of this set of polyhedra also trace back to ancient Greece, where they were studied by Archimedes.<sup>4,6</sup>

One illustrative and relevant example that incorporates both elements of nature's self-assembly processes and its symmetry occurs in the icosahedral or dodecahedral shape of the capsids of most viruses.<sup>2</sup> With their structures elucidated by the modern techniques of X-ray diffraction and electron microscopy, nature has employed these shapes due to their close approximation of a sphere and corresponding maximization of volume to surface area for containing viral genetic information. It has only been in recent times that the tools sophisticated enough to be able to mimic, or attempt to mimic, this biologically inspired strategy of self-assembly have been available. Lacking both the immense time frame and evolutionary selection pressures of nature, however, a more direct methodology had to be formulated.

Clearly, it would be a difficult endeavor to try to use an exact model of nature's process, where multiple *nondirectional* hydrogen-bonding, van der Waals, and other weak interactions are responsible for biological self-assembly. Additionally, stepwise covalent syntheses of large structures are often laborious and generally end in a low overall yield of the desired product. Instead, by utilizing stronger, *directional* metal–ligand dative bonds, the effect of a number of weaker interactions can be encompassed within a single bond, and a much greater handle on abiological self-assembly can be achieved.<sup>7</sup> Coupled with a selective and reasonable choice of precursors, this synthetic strategy allows for the design of a library of large, symmetrical species that mimic not only the overall shape and size of many biological entities but also many of their structural properties and, hopefully in the future, will allow for the potential development of molecules that imitate biological function.

The directional-bonding approach<sup>7f,j,8</sup> to self-assembly has two major requirements at its most basic level. The first calls for rigid, complementary precursors with predefined angles and symmetry for the desired product

S. Russell Seidel graduated summa cum laude with a B.S. in chemistry (ACS) with honors from Washington College in 1997. There, he did his undergraduate thesis with James R. Locker and was the school's awardee for the ACS Maryland Section Student Awards for 1997 and the recipient of the Joseph H. McLain Prize for chemistry. He is currently finishing his doctoral thesis in the research group of Peter J. Stang at the University of Utah, where he was awarded a Henry Eyring Research Fellowship in 1997 and a Dow Chemical Scholarship in 1998.

Peter J. Stang is a Distinguished Professor of Chemistry and the Editor of the *Journal of the American Chemical Society*. He is a member of the U.S. National Academy of Sciences and a fellow of the American Academy of Arts and Sciences.

\* To whom correspondence should be addressed. E-mail: stang@chem.utah.edu. Phone: (801) 581-8329. Fax: (801) 581-8433.

Chart 1. Platonic Solids

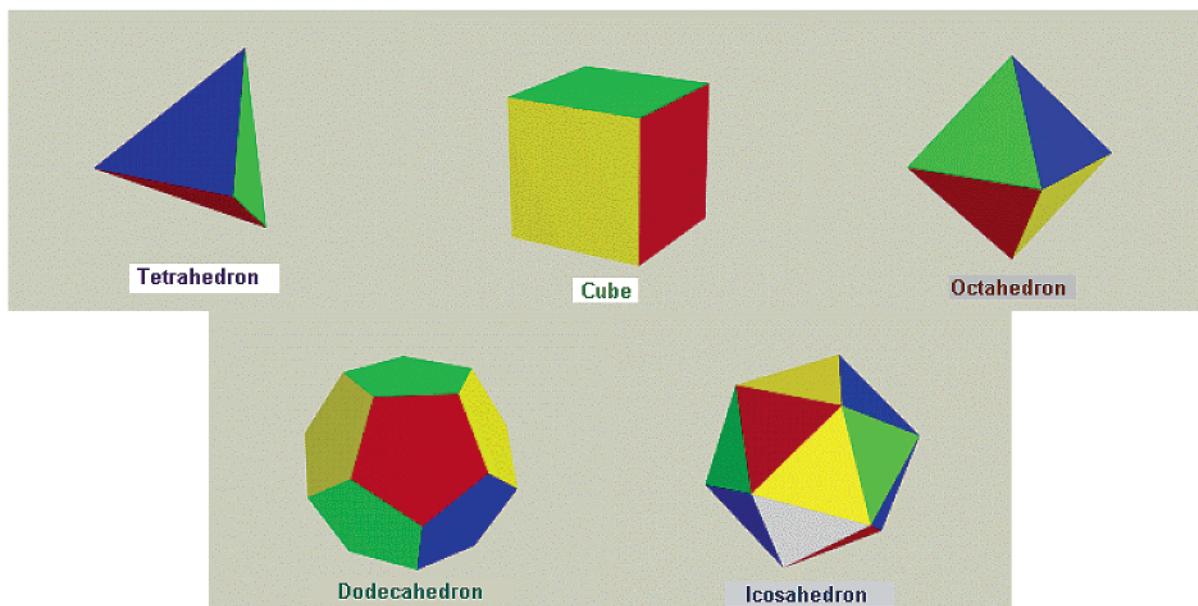
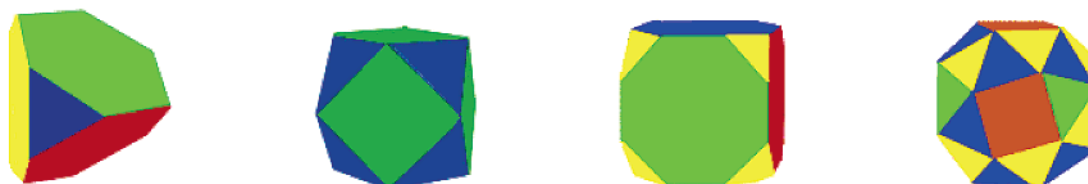


Chart 2. Representative Archimedean Solids: (a) Truncated Tetrahedron, (b) Cuboctahedron, (c) Truncated Cube, and (d) Snub Cube



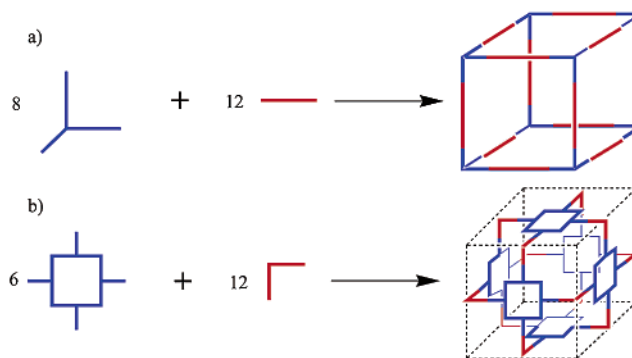
form. The second dictates that the precursors be mixed in the ratios appropriate for the chosen outcome. Practically, however, a number of additional experimental factors influence the process. For instance, the order of precursor addition, the choice of solvent system, the concentration, the temperature, and often even the rate of mixing of the two building blocks have profound influences on the end result of any given self-assembly reaction. Nevertheless, under optimized conditions the yields in these self-assembly processes are generally quantitative within the detection limits of NMR.

In our previous Account,<sup>8</sup> the self-assembly of primarily 2-D systems, such as supramolecular squares and hexagons, was the major focus. Herein, we concentrate exclusively on three-dimensional self-assembly. A variety of supramolecular entities are discussed, as are their structural features, characterization, and preparation, and we demonstrate the viability and general applicability of our directional-bonding<sup>7j</sup> methodology for three-dimensional ensembles.

### General Design Strategies: Edge-Directed vs Face-Directed Self-Assembly

Self-assembly via the directional-bonding approach incorporates two distinct, yet related, methods in the synthesis of supramolecular species. The first is edge-directed self-assembly. As the name implies, precursors whose chemical components will lie upon, and thereby define, the edges of the desired ring or cage are employed.

Scheme 1. (a) Edge-Directed Self-Assembly and (b) Face-Directed Self-Assembly



In this case, the angles present between reactive sites on the building blocks are retained in the final structure and closely match the ideal values for the preferred product. The edge-directed assembly of supramolecular cubes,<sup>9</sup> where 8 tritopic, 90° corner units react with 12 ditopic, linear linkers, serves to illustrate this strategy (Scheme 1a).

The other technique, face-directed self-assembly, is not quite as conceptually apparent. In this paradigm, some or all of the faces of the target aggregate are spanned by the linkers themselves, which hold together the overall architecture. Again, the self-assembly of cubes can provide a reasonable visualization.<sup>10</sup> As shown in Scheme 1b, a face-directed cube can be assembled via the reaction of 6 tetratopic, planar, 90° faces with 12 ditopic, 90° subunits.

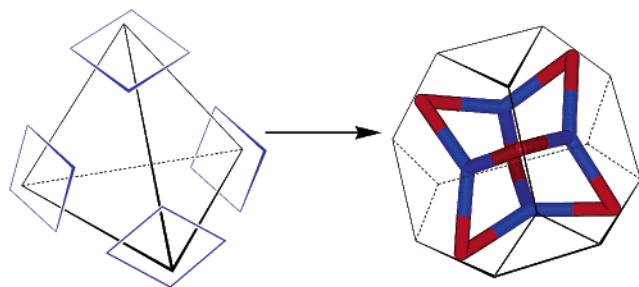


FIGURE 1. Formation of a truncated tetrahedron with inscribed chemical model.

Here, the corners of the cube are missing, while the surfaces are covered.

## Archimedean and Platonic Solids

**Synthetic Hydrocarbons.** Traditional covalent synthesis has yielded cage molecules that possess some of the shapes and/or symmetries of the Platonic solids. Of note have been the syntheses of tetra(*tert*-butyl)tetrahedrane,<sup>11</sup> cubane,<sup>12</sup> and dodecahedrane,<sup>13</sup> that represent the tetrahedron, cube, and dodecahedron, as well as adamantane,<sup>14</sup> whose symmetry is equivalent to the tetrahedron. These molecules are the outcome of a great deal of groundbreaking, difficult work in the field of multistep total synthesis. Other interesting covalent cage compounds include the serendipitously discovered fullerenes.<sup>15</sup>

**Truncated Tetrahedra.** The smallest of the 13 Archimedean solids is the truncated tetrahedron,<sup>5</sup> created by taking the Platonic tetrahedron and truncating, or cutting off, its four corners. This leaves a body consisting of four hexagons and four equilateral triangles (Figure 1).

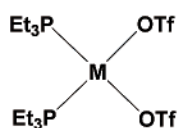
Chemically, a good approximation of this shape can be realized by utilizing four tritopic, planar,  $\sim 120^\circ$  linkers, which span the four hexagonal faces of the truncated tetrahedron in a face-directed manner, clipped together by six ditopic,  $\sim 90^\circ$  subunits. The vertices of these  $\sim 90^\circ$  tectons then serve to outline the triangular surfaces of the polyhedron (Figure 1).<sup>16</sup>

Square planar platinum and palladium compounds, *cis*-(PEt<sub>3</sub>)<sub>2</sub>Pt(OTf)<sub>2</sub> (**1**), *cis*-(PEt<sub>3</sub>)<sub>2</sub>Pd(OTf)<sub>2</sub> (**2**), and *cis*-(PMe<sub>3</sub>)<sub>2</sub>-Pt(OTf)<sub>2</sub> (**3**), and ferrocene-containing linkers **4** and **5**, meet the requirements of the ditopic building block well (Chart 3). For the tritopic, planar counterparts, 1,3,5-tris(4-pyridylethynyl)benzene (**6**), 1,3,5-tris(4-cyanophenylethynyl)benzene (**7**), and 1,3,5-tris(*trans*-4-vinylpyridyl)benzene (**8**) are all viable units (Chart 4).

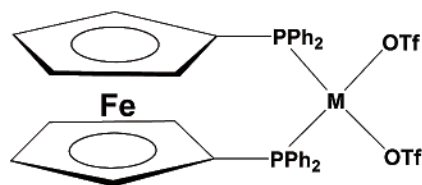
When either **1** or **2** is mixed with **6** in a 3:2 ratio, truncated tetrahedra **9** and **10**, respectively, are the sole products.<sup>16</sup> Similar reactions involving ditopic **4** or **5** with tritopic **6** or **7** result in truncated tetrahedra **11–14**.<sup>16</sup> This latter set of syntheses, which incorporate ferrocene groups at the ditopic corners, have the potential for adding functionality to these cages, such as possible redox chemistry. Moreover, aggregates **15** and **16** can be obtained via the 3:2 mixing of **3** and **6** or **8**, respectively (Scheme 2).<sup>17</sup>

With the intention of testing the modularity of the directional-bonding methodology in this particular system, a complementary truncated tetrahedron can also be prepared. In this case, when ditopic,  $\sim 90^\circ$  donor unit **17**, a bis(pyridyl)porphyrin (Chart 3), is reacted in the appropriate ratio with tritopic, planar,  $\sim 120^\circ$  platinum

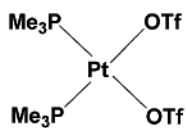
Chart 3. Ditopic Corners



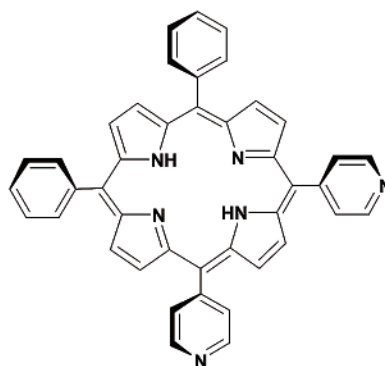
1: M = Pt  
2: M = Pd



4: M = Pd  
5: M = Pt

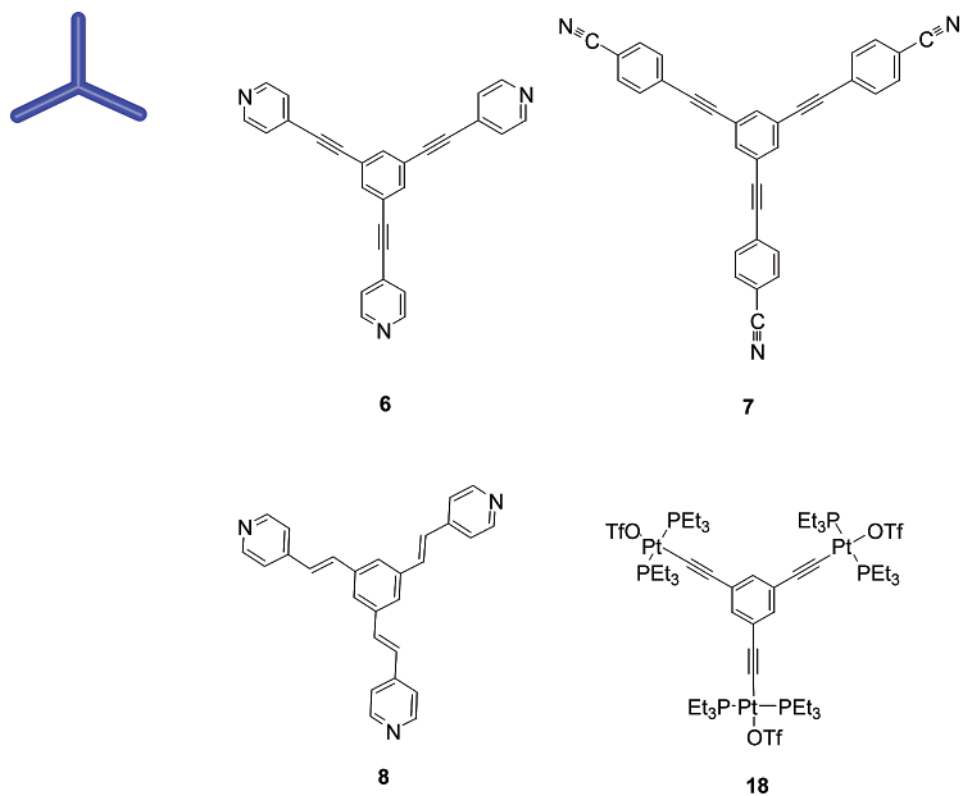


3

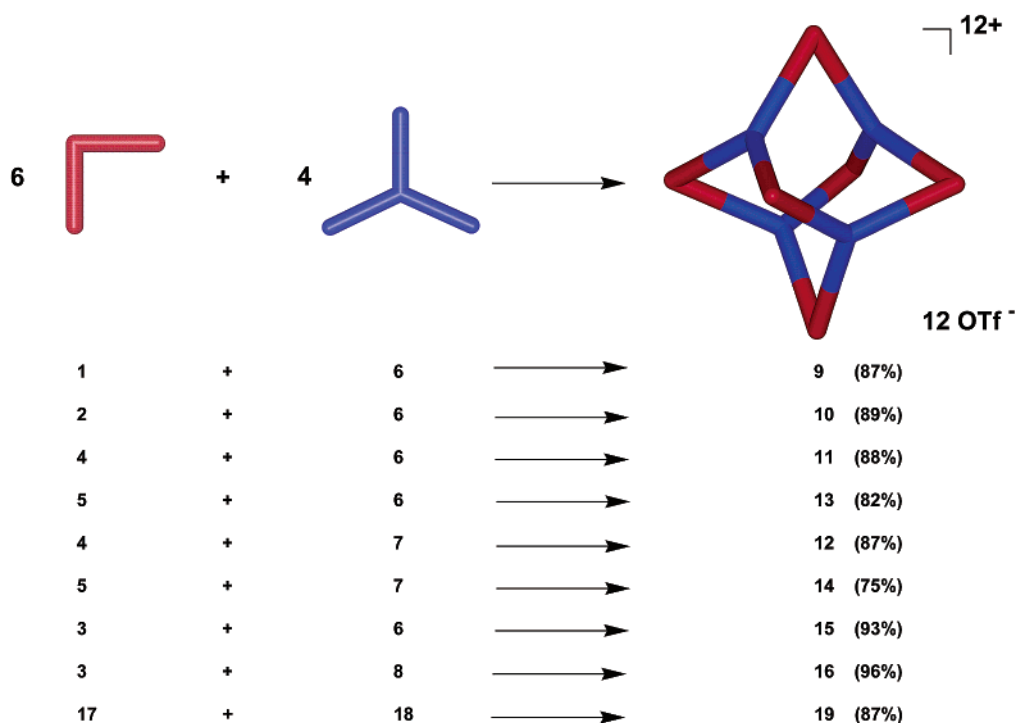


17

Chart 4. Planar Tritopic Linkers



Scheme 2. Self-Assembly of Truncated Tetrahedra



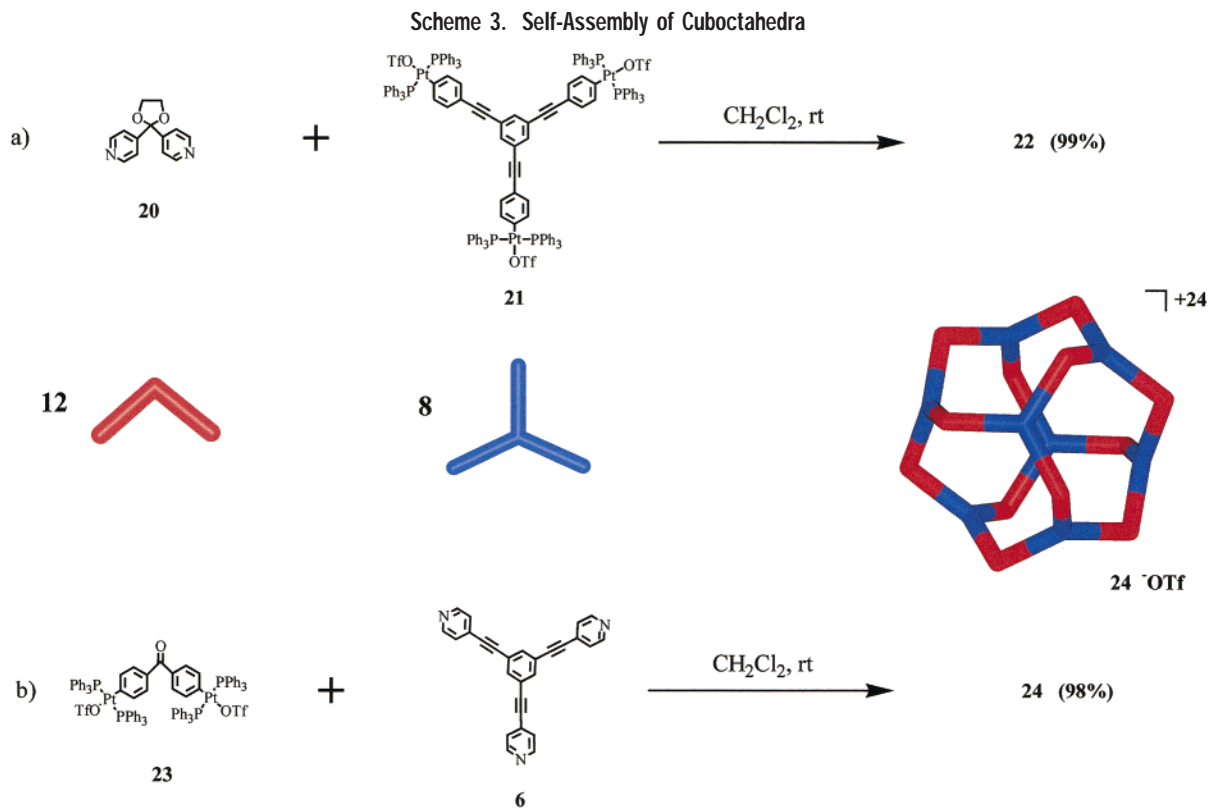
acceptor unit **18** (Chart 4), a cage compound (**19**) analogous to the previous eight is realized (Scheme 2).<sup>16</sup>

Polyhedra **9–16** and **19** are all characterized by multinuclear NMR, showing products of high symmetry. All but **12** and **14**, which contain the weaker cyano–metal dative bonds and exhibit no MS data at all, and **15** and **16**, which

are still under investigation, show electrospray ionization mass spectrometry (ESI-MS) fragmentation patterns and molecular ions consistent with the stated product structure.

Extensible systematic force field (ESFF) calculations<sup>18</sup> have been employed in the molecular modeling of trun-

## Scheme 3. Self-Assembly of Cuboctahedra



cated tetrahedron **12**. This model shows a palladium-to-palladium cross-cavity distance of approximately 2.2 nm, and an overall diameter of roughly 3.5 nm for **12**.<sup>16</sup> Furthermore, preliminary single-crystal X-ray structures of **15** and **16** have been obtained and correspond with the proposed truncated tetrahedral structures.<sup>17</sup>

**Cuboctahedra.** Another interesting Archimedean solid is the cuboctahedron.<sup>5</sup> This structure is made up of six square faces and eight equilateral triangular faces, and thereby possesses features of both the Platonic cube and octahedron (Figure 2).<sup>4</sup> Overall it has 12 vertices, 24 edges, and a dihedral angle between the triangular and the square surfaces of 125°. <sup>6</sup>

A good approximation of a cuboctahedron can be achieved chemically by making use of the face-directed design strategy. When a 108° ditopic tecton is reacted with a complementary<sup>19</sup> planar, tritopic, 120° building block in a 12:8 ratio, respectively, a cuboctahedral cage results. The tritopic linkers span the eight triangular faces and are clipped together by the ditopic linkers, whose vertices then serve to outline the six square surfaces (Figure 2).

Acting as a reasonable approximation of the ditopic component is ~109.5° donor subunit **20**, 4,4'-bispyridylacetal, while ~120° platinum acceptor unit **21**, which is similar to compound **18** used in the preparation of the truncated tetrahedra above, meets the requisite criteria for the tritopic component. When these two building blocks are mixed in a 3:2 ratio, respectively, cuboctahedron **22** results (Scheme 3).<sup>19</sup>

Similar to the truncated tetrahedra, a complementary cuboctahedron, where the donor and acceptor sites are switched between ditopic and tritopic tectons, can also

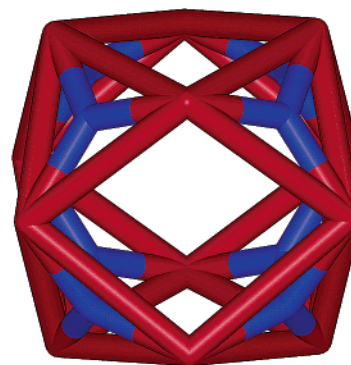
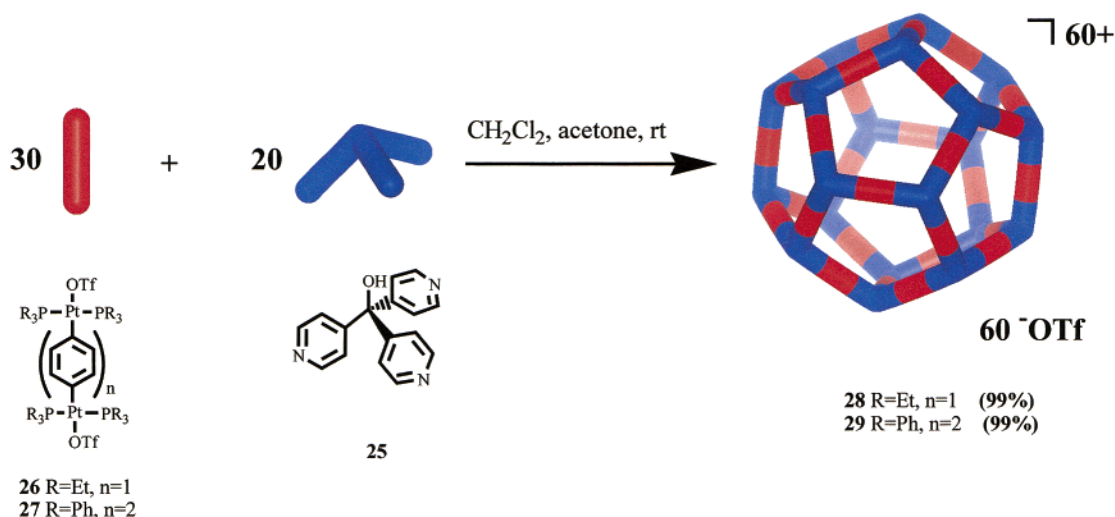


FIGURE 2. Cuboctahedron with chemical model frame.

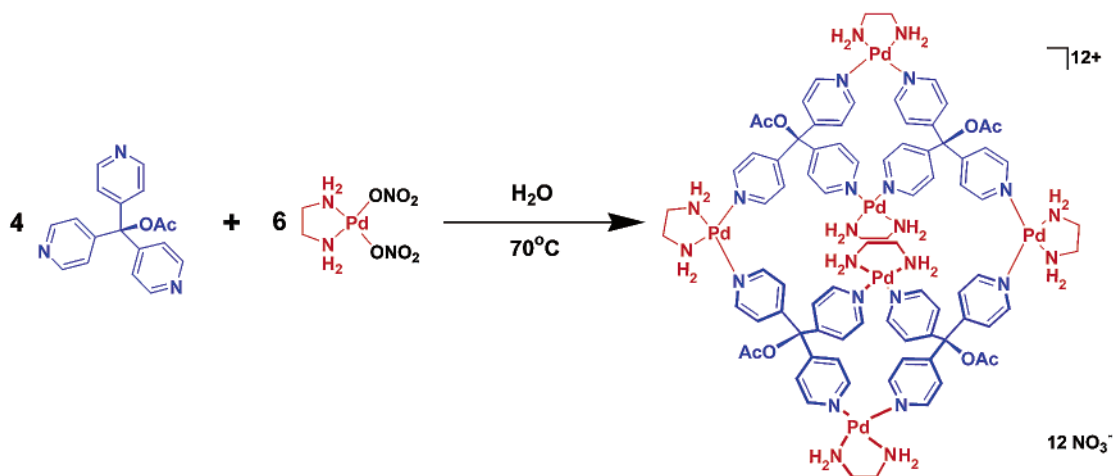
be prepared. Taking the role of the ditopic entity is ~120° acceptor unit **23**, bis(4-[*trans*-Pt(PPh<sub>3</sub>)<sub>2</sub>OTf]phenyl)ketone, while the tritopic task is assumed by planar, ~120° linker **6**. Despite **23**'s angular deviation from the ideal<sup>19</sup> 108° angle necessary for the cuboctahedron, the reaction of the two linkers under conditions similar to those for **22** affords cuboctahedron **24** (Scheme 3).<sup>19</sup>

Both **22** and **24** are characterized by multinuclear NMR, which are indicative of a highly symmetrical species in each case, elemental analysis, and ESI-MS, giving peaks that correspond to the presumed structures, less a given number of triflates, and their fragments. Furthermore, the pulsed gradient spin-echo (PGSE) NMR technique<sup>20</sup> shows a self-diffusion coefficient of  $(1.92 \pm 0.072) \times 10^{-6} \text{ cm}^2 \text{ s}^{-1}$  at 25 °C, providing a hydrodynamic diameter of 5.0 nm for cuboctahedron **24**. This value is consistent with an ESFF<sup>18</sup> molecular model of **24**, making it one of the largest self-assembled species (MW = ~26 000) to date.<sup>19</sup> Additionally, these highly charged, organic-soluble species

Scheme 4. Self-Assembly of Dodecahedra



Scheme 5. Self-Assembly of Fujita's Double-Square Architecture



represent, to the best of our knowledge, the first man-made, self-assembled entities with *O* symmetry.

**Dodecahedra.** The dodecahedron, consisting of 12 regular pentagonal faces, represents the second largest of the Platonic solids. With its  $I_h$  point group, which is identical to that of the coats of icosahedral-shaped viruses,<sup>2</sup> it has a higher degree of symmetry than the three smaller Platonic bodies.<sup>5</sup> The tetrahedra,<sup>21</sup> cubes,<sup>9,10</sup> and octahedra<sup>22</sup> have all been realized as the results of an array of elegant research by various innovators in the field of self-assembly. For instance, Raymond and co-workers have produced multiple tetrahedra based on a chelation paradigm,<sup>21</sup> while the research of Thomas has yielded an edge-directed cube,<sup>9a</sup> and that of Grieco has been responsible for a face-directed analogue.<sup>10</sup> Fujita and co-workers have reported several examples of self-assembled octahedra.<sup>22</sup>

In the synthesis of a macromolecular dodecahedral cage, an edge-directed approach has proven effective.<sup>23</sup> This strategy requires the self-assembly of 50 building blocks, 30 of which consist of ditopic,  $\sim 180^\circ$  edges and the other 20 comprise tritopic,  $\sim 108^\circ$  vertices. Both of these precursor geometries are readily available in chem-

istry, with the linear units being attainable from para-substituted phenyl rings and the tritopic units accessible in the form of tetrahedral carbon atoms incorporating the proper substituents.

Tris(4-pyridyl)methanol (**25**) has all of the attributes necessary to function as the tritopic vertex, as shown by way of its single-crystal X-ray structure (Figure 3a), while bis[1,4-(*trans*-Pt(PEt<sub>3</sub>)<sub>2</sub>OTf)]benzene (**26**, Figure 3b) and the longer bis[4,4'-(*trans*-Pt(PPh<sub>3</sub>)<sub>2</sub>OTf)]biphenyl (**27**) fulfill those of the ditopic edge unit. The reaction of **25** with either **26** or **27** yields dodecahedra **28** and **29**, respectively (Scheme 4).<sup>23</sup>

Dodecahedra **28** and **29** are characterized by multinuclear NMR, again showing the overall assemblies as entities of high symmetry, and ESI-MS data, which give both parent peaks, with the corresponding loss of triflate anions, and fragmentation patterns consistent with the proposed macromolecular aggregates.<sup>23</sup>

While the definitive proof provided by an X-ray structure could not be obtained to date, most likely due to the size and high symmetry of such entities, two additional methods of product elucidation provide strong evidence for the structural assignment. The first, as used previously

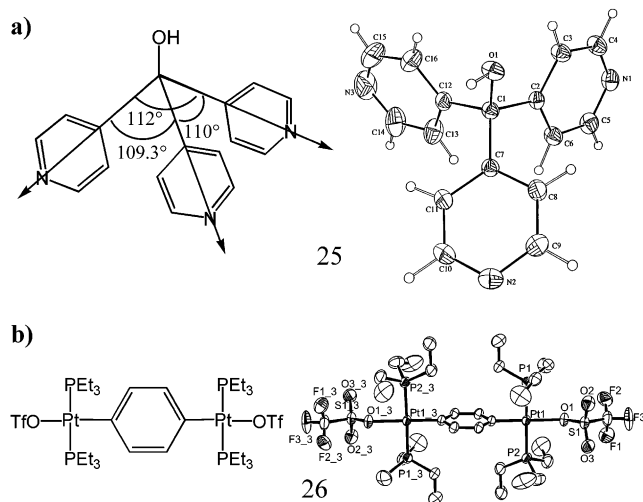


**FIGURE 3.** (a) ORTEP plot of tris(4-pyridyl)methanol (**25**). (b) ORTEP plot of bis[1,4-(*trans*-Pt(PEt<sub>3</sub>)<sub>2</sub>OTf)]benzene (**26**).

with cuboctahedron **24**, is the PGSE NMR technique.<sup>20</sup> Cage **28** gives a self-diffusion coefficient of  $(1.80 \pm 0.05) \times 10^{-6} \text{ cm}^2 \text{ s}^{-1}$ , while **29** gives that of  $(1.32 \pm 0.06) \times 10^{-6} \text{ cm}^2 \text{ s}^{-1}$ , both at 25 °C, leading to hydrodynamic diameters of 5.2 and 7.5 nm, respectively. These are in accord with the predicted sizes for dodecahedra of these chemical compositions. Furthermore, transmission electron microscopy (TEM) performed on **29** exhibits particles of roughly the correct shape and size ( $\sim 8$  nm across) when deposited on a thin carbon film at high dilution (Figure 4).<sup>23</sup>

With their molecular masses of  $\sim 41\,000$  (C<sub>1220</sub>H<sub>2180</sub>N<sub>60</sub>-P<sub>120</sub>S<sub>60</sub>O<sub>200</sub>F<sub>180</sub>Pt<sub>60</sub>) for **28** and  $\sim 62\,000$  (C<sub>2900</sub>H<sub>2300</sub>N<sub>60</sub>P<sub>120</sub>S<sub>60</sub>-O<sub>200</sub>F<sub>180</sub>Pt<sub>60</sub>) for **29**, these two organic-soluble dodecahedra are among the largest high-symmetry transition-metal-based, discrete assemblies that have been artificially constructed to date. Their nanoscopic void spaces, which are occupied by solvents and/or anions, are potentially capable of fitting an array of large guests, and the sheer size of these entities falls within the domain of proteins.

## Other Coordination Cages

**Trigonal Bipyramids.** A trigonal bipyramid consists of two pyramids stacked on top of one another in such a way as to create a six-faced solid belonging to the *D*<sub>3h</sub> symmetry point group. The faces of an entity of this sort are all triangular.

One can conceive of synthesizing an edge-directed supramolecular trigonal bipyramid by clipping together two tritopic, tetrahedral donors with three ditopic,  $\sim 90^\circ$ , square planar acceptors. Such a reaction, however, resulted instead in the formation of an intriguing, heretofore unknown double square architecture when put into practice by Fujita and co-workers (Scheme 5).<sup>24</sup>

Clearly, the design strategy itself would have to be manipulated if one were to obtain a trigonal bipyramid from a reaction of this sort. A large deviation would be required to take rigid building blocks, such as those utilized by Fujita and co-workers, and distort them into

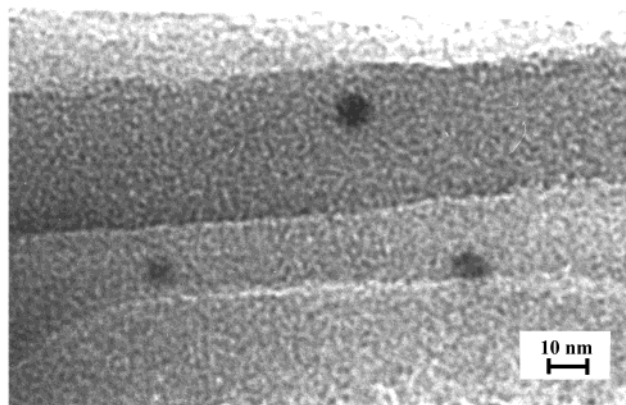


**FIGURE 4.** TEM micrograph of the larger dodecahedron **29**.

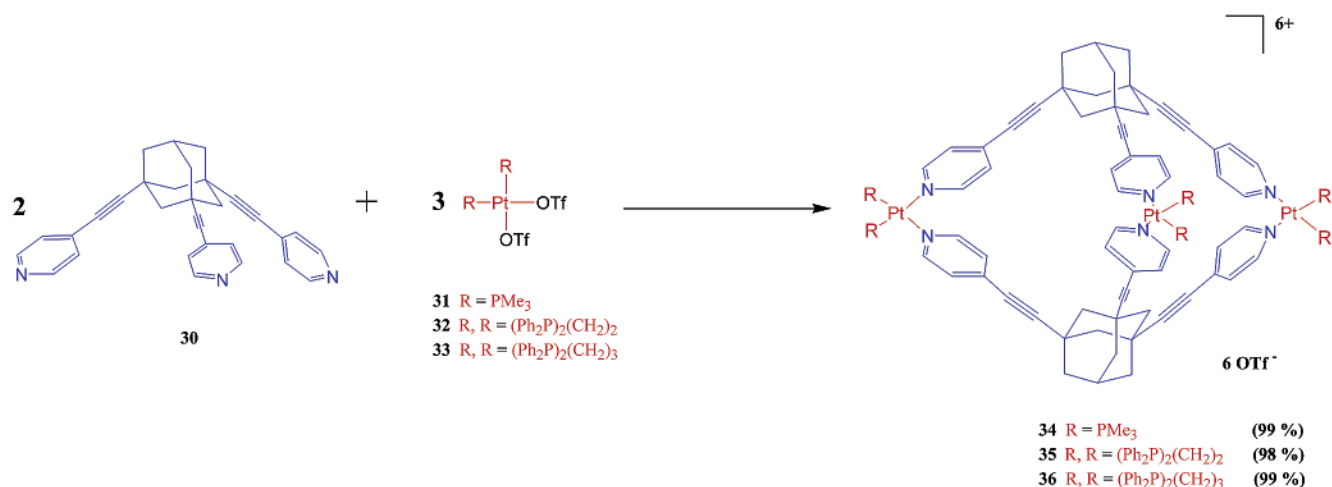
the smaller assembly. The double square thus represented a balance between entropy, where the smallest structure is favored, and enthalpy, where the structure with the least strain is prevalent.

Recognizing this fact, however, the design can be manipulated in such a way as to tip the thermodynamic factors in favor of a trigonal bipyramid. For instance, if enough flexibility is incorporated into the tritopic,  $\sim 109^\circ$  tecton, as is the case with (adamantyl/ethynyl)-containing tris(pyridyl) linker **30**, the reaction with generic, ditopic,  $\sim 90^\circ$  platinum(II) subunits, such as **31–33**, can feasibly provide a large enough framework for strain delocalization, allowing a trigonal bipyramidal cage to be produced. Indeed, when such reactions are carried out in a 2:3 ratio, trigonal bipyramids **34**, **35**, and **36** result, respectively (Scheme 6).<sup>25</sup> Lacking an X-ray structure, the identity of these trigonal bipyramids can be differentiated from that of double squares by multinuclear NMR spectroscopy. Due to reduced symmetry, double squares have two distinct sets of signals in their <sup>1</sup>H NMR, for their pyridyl protons,<sup>24</sup> and their <sup>31</sup>P NMR spectra, in a ratio of 2:1. Trigonal bipyramidal entities of the sort presented here should have only a single set of pyridyl signals in the proton spectrum and a singlet with <sup>195</sup>Pt satellites in the phosphorus spectrum as a result of the symmetry equivalence of their equatorial positions; **34–36** do. Additionally, ESI-MS data for **35** and **36** correspond to the trigonal bipyramid structure, as do those for **34**, after two of its triflate anions are exchanged for cobalticboranes.<sup>25</sup>

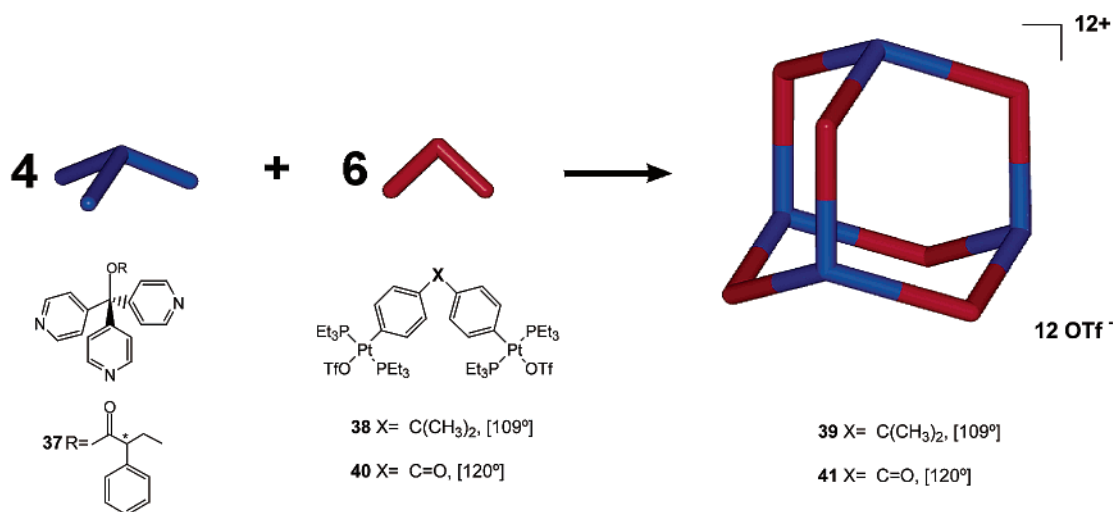
**Adamantanoids.** Discovered in the 1930s,<sup>14</sup> adamantane is one of the most stable hydrocarbons. This high degree of stability is due to its arrangement of four cyclohexane rings fused with each in the favorable chair conformation. As a consequence of this stability, it can be produced catalytically from a wide variety of precursor organic substances, as shown by Schleyer and co-workers.<sup>14c</sup> The adamantanoid unit is also the simplest element of the diamond lattice.

Adamantane exhibits a shape similar to a tetrahedron that has had its edges kinked into  $109.5^\circ$  angles at their points of bisection. While these distortions cause the sides and angles to deviate from those of a tetrahedron, adamantane retains its overall symmetry, that of point group *T<sub>d</sub>*. Unlike the previous entities reported thus far,

Scheme 6. Self-Assembly of Trigonal Bipyramids



Scheme 7. Self-Assembly of Adamantanoids



which have their roots in solid geometry, the adamantanoid is a purely chemistry-derived species.

Self-assembled adamantanoids were first introduced by Saalfrank and co-workers, utilizing a different, chelation-based paradigm.<sup>26</sup> Nanoscopic adamantanoids can be designed according to the directional-bonding approach by adopting an edge-directed strategy. Since the shape itself consists of four fused, chair-conformed cyclohexane-like rings, a quick examination of the structure reveals that all of the pertinent angles should be 109.5°, which matches the ideal tetrahedral geometry of  $\text{sp}^3$ -hybridized carbon atoms (Figure 5). This allows for a number of possible building blocks from the chemical world.

Employing chiral, tritopic,  $\sim 109.5^\circ$  donor subunit **37**, a derivative of tris(4-pyridyl)methanol (**25**), in reaction with ditopic,  $\sim 109.5^\circ$  acceptor subunit **38**, both of which meet the requirements for the adamantanoid superstructure, leads to the desired cage **39** (Scheme 7).<sup>27</sup> To investigate the stringency of the design strategy, an  $\sim 120^\circ$  analogue of **38**, building block **40**, can also be utilized in a similar, 6:4 reaction with tecton **37**. As was the case with cuboctahedron **24**, where a similar idea was explored, adamantanoid **41** indeed results (Scheme 7).<sup>27</sup>

Cages **39** and **41** are characterized by multinuclear NMR, which indicates a highly symmetrical species, and ESI-MS and elemental analysis data that correspond to the proposed structures. An MM2 force field<sup>28</sup> model of **39** exhibits an inner void which is  $\sim 3$  nm across (Figure 6).<sup>27</sup>

Additionally, since tritopic building block **37** contains a stereogenic center ( $[\phi]_D = -122$ ), both **39** and **41** are themselves optically active ( $[\phi]_D = -261$  and  $-1168$ , respectively).<sup>27</sup> This reduces the overall symmetry of the two chiral aggregates to  $D_2$  from the achiral expectation of  $T_d$ .

**Trigonal Prisms.** Belonging to the  $D_{3h}$  point group, trigonal prisms represent a class of polyhedra that are of equivalent symmetry to the trigonal bipyramids presented earlier and of lower symmetry than the Archimedean and Platonic solids already examined. To chemically approximate a trigonal prism,<sup>29</sup> a face-directed design strategy holds great appeal. In this approach, three ditopic organometallic clips, which each possess two nearly parallel bonding sites separated by a linear chemical framework, can be reacted with two ideally  $120^\circ$ , tritopic, planar subunits.<sup>30,31</sup> In such systems, the tritopic units



Scheme 8. Self-Assembly of Nondistorted Trigonal Prisms

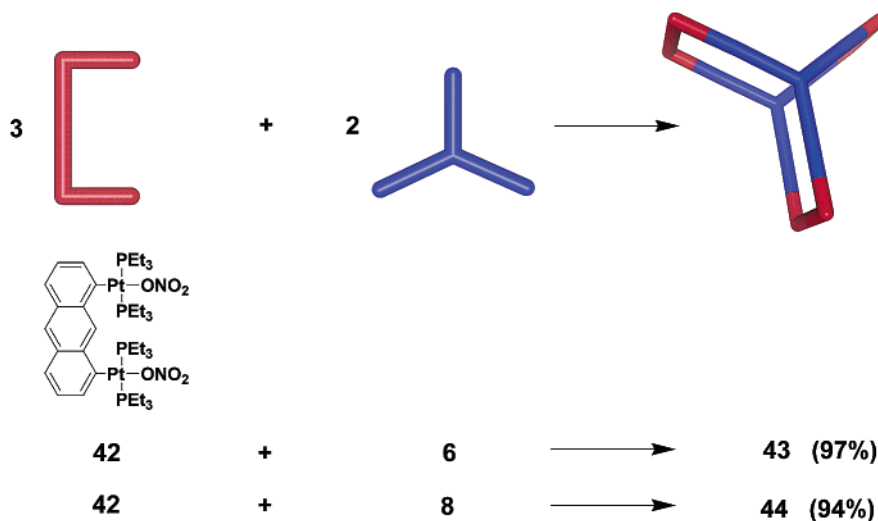


Chart 5. Tritopic Tetrahedral Linker 45

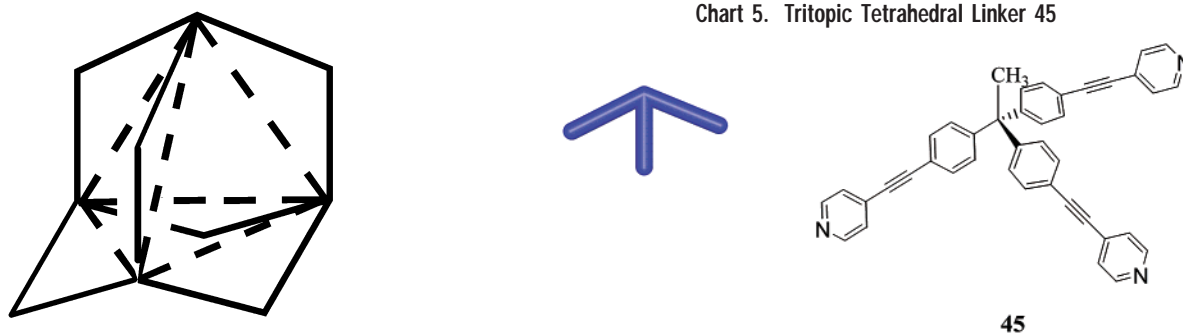


FIGURE 5. Adamantanoid shape with inscribed tetrahedron.

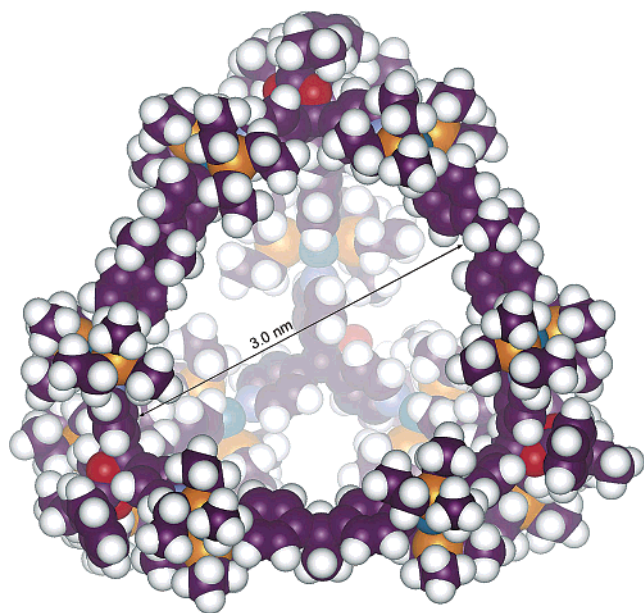


FIGURE 6. MM2 model of adamantanoid 39.

span the triangular faces of the prism, as they are clipped together by the ditopic units. The vertices of the clips then serve to outline the rectangular faces.

Reaction of planar, tritopic tecton **6** or its tris(ethylene) analogue **8** with ditopic, acceptor building block **42**, which has already proven itself as an effective clip in similar two-

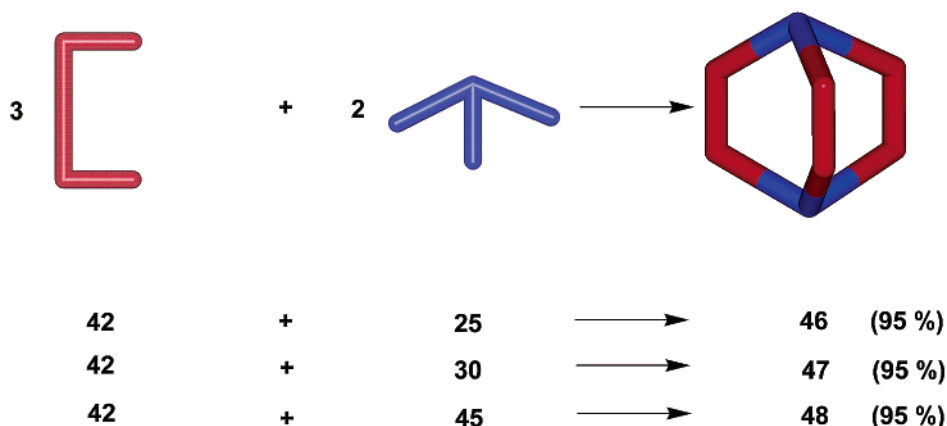
dimensional rectangular species,<sup>32</sup> provides the desired trigonal prismatic cages **43** and **44**, respectively (Scheme 8).<sup>30</sup>

As in the successful formation of cuboctahedron **24** and adamantanoid **41**, the leniency of the design methodology can be put to the test. In so doing, tritopic, *nonplanar*,  $\sim 109^\circ$  linkers, tris(4-pyridyl)methanol (**25**), adamantyl/ethynyl-containing tris(pyridyl) subunit **30**, and extended building block **45** (Chart 5), yield related, somewhat distorted trigonal prisms **46**, **47**, and **48**, respectively, with clip **42** (Scheme 9).<sup>31</sup>

After precipitation and anion-exchange with  $\text{KPF}_6$ , the multinuclear NMR spectra for polyhedra **43**, **44**, **46**–**48** all exhibit signals consistent with highly symmetrical entities, while the elemental analysis data for each correspond well to the theoretical values. This occurs even in the case of **46**, which underwent incomplete exchange, leaving a nitrate anion bound in its cage. ESI-MS data strongly support the presumed structures of all five trigonal prisms and, indeed, show the presence of the nitrate guest in **46**.<sup>30,31</sup>

Single-crystal X-ray crystallography firmly establishes the structure of cages **46** and **48**. The structure of **46** gives a trigonal prism that is  $\sim 1 \text{ nm} \times 2 \text{ nm}$  and establishes that the nitrate is included in the cationic host (Figure 7a), while that of **48** provides a much larger,  $\sim 1 \text{ nm} \times 4 \text{ nm}$  assembly (Figure 7b).<sup>31</sup>

## Scheme 9. Self-Assembly of Distorted Trigonal Prisms



## Host–Guest Chemistry

Although still in the developmental stages, a number of instances of host–guest chemistry for three-dimensional coordination cages have been reported in the literature over the past few years. Among these is our example of nitrate encapsulation, both in the solid state and in solution, by the cationic trigonal prismatic host **46**.<sup>31</sup>

Utilizing water-soluble octahedra, which can also be viewed as truncated tetrahedra, Fujita and co-workers have produced much research into the potential uses of three-dimensional self-assembled aggregates.<sup>22</sup> Such compounds have been employed in the entrapment of sizable neutral molecules, including *o*-carborane and adamantane.<sup>22a</sup> For both *o*-carborane and adamantane, a host-to-guest ratio of 1:4 was realized, showing no signs of intermediate ratios, even when the guest, in the case of *o*-carborane, was introduced at a lower than ideal percentage. The hydrophobic cavity of the cage was believed to be in large part responsible for the inclusion phenomena, and characterization was carried out via NMR studies.

Such species have also been employed in forming stable *cis*-azobenzene and *cis*-stilbene derivative dimers within their cavities.<sup>22b</sup> Molecular modeling and NMR evidence showed that these enclathrated molecules adopted the dimerized form in a selective, “ship-in-a-bottle” fashion instead of forming prior to encapsulation. The guest–guest baseball-like shape was supported by NOE experiments, while the specifics of the host–guest complexes were established by NMR.

A similar experiment was conducted in which this “ship-in-a-bottle” motif was exploited in the isolation of typically transitory cyclotrimers of various silanols.<sup>22f</sup> These species, which are important intermediates in sol-gel condensation reactions, could be prepared within the hydrophobic cavities of the cage from their constituent aryltrimethoxysilane precursors. While the precursors were small enough to move freely through the portals of the assembly, their condensation product was not, and it became trapped upon being formed within the supramolecular aggregate’s void space. The host–guest species were characterized by NMR and ESI-MS.

Additionally, a molecular “lock” based on these compounds has been prepared which can be thermally

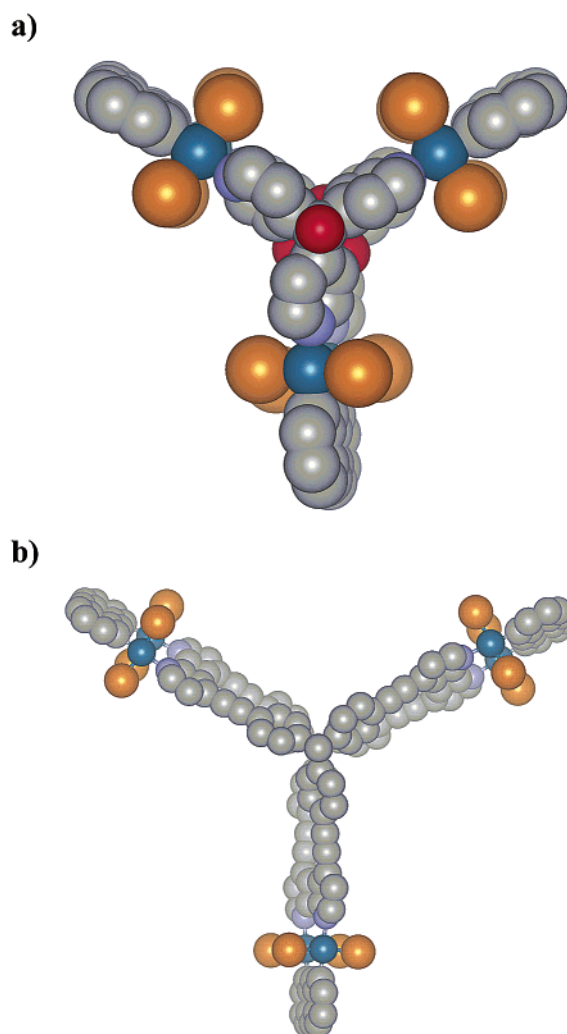


**FIGURE 7.** (a) Smaller trigonal prism **46** (based on XRD data; CPK model). (b) Larger trigonal prism **48** (based on XRD data; CPK model). Hydrogen atoms and ethyl groups are omitted from both models for clarity.

switched.<sup>22c</sup> The synthesis of a platinum(II) octahedron occurred readily upon heating an originally oligomeric mixture of the precursor building blocks in D<sub>2</sub>O at 100 °C and in the presence of a template, sodium adamantanecarboxylate. The Pt–N bond, which was labile at the elevated temperature, became inert when the mixture was

cooled, resulting in a locking of the cage complex. This locked structure was found to be highly pH-resilient, allowing for the development of a pH-dependent host–guest system in which *N,N*-dimethylaniline could be removed from the cavity under acidic conditions and put back under basic conditions.

Further examples<sup>7f</sup> of host–guest chemistry have been detailed in supramolecular assemblies based on the “symmetry interaction” paradigm of Saalfrank and Raymond. These instances are evidenced by Saalfrank’s mixed-valence iron-based adamantanoid,<sup>26b</sup> which proved an effective host for ammonium cations, and by Raymond’s similar, tetrahedral iron and gallium clusters,<sup>21c,d</sup> the former of which encapsulated an Et<sub>4</sub>N<sup>+</sup> cation and was characterized by X-ray crystallography, and the latter of which was used in NMR-based guest-exchange studies with Et<sub>4</sub>N<sup>+</sup>, Me<sub>4</sub>N<sup>+</sup>, and Pr<sub>4</sub>N<sup>+</sup>. These studies showed that the Pr<sub>4</sub>N<sup>+</sup> could quickly and completely displace Me<sub>4</sub>N<sup>+</sup> from the cavity, while Et<sub>4</sub>N<sup>+</sup> could do the same to the Pr<sub>4</sub>N<sup>+</sup> guest. Equilibrium constants for the Pr<sub>4</sub>N<sup>+</sup> and the Et<sub>4</sub>N<sup>+</sup> relative to K<sup>+</sup> were calculated, and an approximately 200-fold difference in favor of the Et<sub>4</sub>N<sup>+</sup> cations as encapsulated species was found. The disparity was even greater when the Me<sub>4</sub>N<sup>+</sup> ions were the guests.

## Conclusion and Outlook

By employing transition-metal-mediated, coordination-driven self-assembly in the synthesis of nanoscopic Archimedean solids, such as truncated tetrahedra and cuboctahedra, Platonic solids, like the dodecahedron, and numerous other cages, such as trigonal bipyramids, adamantanoids, and trigonal prisms, we have succeeded in expanding the directional-bonding methodology into the realm of three-dimensional architectures. These nanoscopic complexes, whose sizes can even extend into the range of small proteins, have large internal cavities that offer an array of future possibilities, such as catalysis and the inclusion of large molecules, biomolecules, particles, etc. Additionally, with the dimensional and functional variety accessible from this modular approach, a multitude of other, more long-term goals can be envisioned, including in the areas of nanomachinery and perhaps even the actual imitation of biological function.

*This Account is dedicated to Professor Robert W. Parry on the occasion of his 85th birthday. We thank our co-workers and collaborators, as given in the references, for their dedication and diligent efforts for making it all work. We are also grateful to Yuri Kryschenko for his assistance with the graphics and to the NSF (CHE-9818472) and the NIH (5R01GM57052) for financial support.*

## References

- (1) *Self-Assembling Architecture*; Varner, J. E., Ed.; Alan R. Liss: New York, 1988.
- (2) (a) Horne, R. W. *Virus Structure*; Academic Press: New York, 1974. (b) Cann, A. J. *Principles of Molecular Virology*; Academic Press: San Diego, 1993; pp 1–234.
- (3) Cooper, J. A. Self-Assembly of Actin Filaments. In *Self-Assembling Architecture*; Varner, J. E., Ed.; Alan R. Liss: New York, 1988; pp 171–177.
- (4) Wenninger, M. J. *Polyhedron Models*; Cambridge University Press: New York, 1970.
- (5) MacGillivray, L. R.; Atwood, J. L. Structural Classification and General Principles for the Design of Spherical Molecular Hosts. *Angew. Chem., Int. Ed.* **1999**, *38*, 1018–1033.
- (6) Pugh, A. *Polyhedra: A Visual Approach*; University of California Press: Los Angeles, 1976.
- (7) (a) Lehn, J.-M. *Supramolecular Chemistry Concepts and Perspectives*; VCH: Weinheim, 1995; pp 139–160. (b) Chambron, J.-C.; Dietrich-Buchecker, C.; Sauvage, J.-P. Transition Metals as Assembling and Templating Species: Synthesis of Catenanes and Molecular Knots. In *Comprehensive Supramolecular Chemistry*; Lehn, J.-M., Atwood, J. L., Davies, J. E. D., MacNicol, D. D., Vogtle, F., Eds.; Pergamon: Oxford, 1996; Vol. 9, pp 43–83. (c) Piguet, C.; Bernardinelli, G.; Hopfgartner, G. Helicates as Versatile Supramolecular Complexes. *Chem. Rev.* **1997**, *97*, 2005–2062. (d) Caulder, D. L.; Raymond, K. N. Supermolecules by Design. *Acc. Chem. Res.* **1999**, *32*, 975–982. (e) Caulder, D. L.; Raymond, K. N. The rational design of high-symmetry coordination clusters. *J. Chem. Soc., Dalton Trans.* **1999**, 1185–1200. (f) Leininger, S.; Olenyuk, B.; Stang, P. J. Self-Assembly of Discrete Cyclic Nanostructures Mediated by Transition Metals. *Chem. Rev.* **2000**, *100*, 853–908. (g) Swieggers, G. F.; Malefsette, T. J. New Self-Assembled Structural Motifs in Coordination Chemistry. *Chem. Rev.* **2000**, *100*, 3483–3538. (h) Saalfrank, R. W.; Uller, E.; Demleitner, B.; Bernt, I. Synergistic Effect of Serendipity and Rational Design in Supramolecular Chemistry. In *Structure and Bonding*; Fujita, M., Ed.; Springer: Berlin, 2000; Vol. 96, pp 149–175. (i) Fujita, M.; Umemoto, K.; Yoshizawa, M.; Fujita, N.; Kusakawa, T.; Biradha, K. Molecular paneling via coordination. *Chem. Commun.* **2001**, 509–518. (j) Holliday, B. J.; Mirkin, C. A. Strategies for the Construction of Supramolecular Compounds through Coordination Chemistry. *Angew. Chem., Int. Ed.* **2001**, *40*, 2022–2043. (k) Cotton, F. A.; Lin, C.; Murillo, C. A. Supramolecular Arrays Based on Dimetal Building Units. *Acc. Chem. Res.* **2001**, *34*, 759–771.
- (8) Stang, P. J.; Olenyuk, B. Self-Assembly, Symmetry, and Molecular Architecture: Coordination as the Motif in the Rational Design of Supramolecular Metallacyclic Polygons and Polyhedra. *Acc. Chem. Res.* **1997**, *30*, 502–518.
- (9) (a) Roche, S.; Haslam, C.; Adams, H.; Heath, S. L.; Thomas, J. A. Self-assembly of a supramolecular cube. *Chem. Commun.* **1998**, 1681–1682. For related compounds, see: (b) Klausmeyer, K. K.; Rauchfuss, T. B.; Wilson, S. R. Stepwise Assembly of [(C<sub>5</sub>H<sub>5</sub>)<sub>4</sub>(C<sub>5</sub>-Me)<sub>4</sub>Co<sub>4</sub>Rh<sub>4</sub>(CN)<sub>12</sub>]<sup>4+</sup>, an “Organometallic Box”. *Angew. Chem., Int. Ed.* **1998**, *37*, 1694–1696. (c) Contakes, S. M.; Klausmeyer, K. K.; Milberg, R. M.; Wilson, S. R.; Rauchfuss, T. B. The Seven-Component Assembly of the Bowl-Shaped Cages Cp\*<sub>7</sub>Rh<sub>7</sub>(CN)<sub>12</sub><sup>2+</sup> and Cp\*<sub>7</sub>Rh<sub>3</sub>Ir<sub>4</sub>(CN)<sub>12</sub><sup>2+</sup>. *Organometallics* **1998**, *17*, 3633–3635. (d) Klausmeyer, K. K.; Wilson, S. R.; Rauchfuss, T. B. Alkali Metal-Templated Assembly of Cyanometalate “Boxes” (NEt<sub>4</sub>)<sub>3</sub>[M(Cp\*<sub>7</sub>Rh(CN)<sub>3</sub>]<sub>4</sub>[Mo(CO)<sub>3</sub>]<sub>4</sub>] (M = K, Cs). Selective Binding of Cs<sup>+</sup>. *J. Am. Chem. Soc.* **1999**, *121*, 2705–2711.
- (10) Johannessen, S. C.; Brisbois, R. G.; Fischer, J. P.; Grieco, P. A.; Counterman, A. E.; Clemmer, D. E. A Nano-Scale Barrel and Cube: Transition Metal-Mediated Self-Assembly of CpCoCb-Derived Ligand Scaffolds. *J. Am. Chem. Soc.* **2001**, *123*, 3818–3819.
- (11) Maier, G.; Pfriem, S.; Schaefer, U.; Matusch, R. Tetra-*tert*-butyltetrahedrane. *Angew. Chem., Int. Ed. Engl.* **1978**, *17*, 520–521.
- (12) (a) Eaton, P. E.; Cole, F. W. Cubane. *J. Am. Chem. Soc.* **1964**, *86*, 3157–3158. (b) Fleischer, E. B. X-Ray Structure Determination of Cubane<sup>1</sup>. *J. Am. Chem. Soc.* **1964**, *86*, 3889–3890.
- (13) (a) Paquette, L. A.; Ternansky, R. J.; Balogh, D. W. A strategy for the synthesis of monosubstituted dodecahedrane and the isolation of an isododecahedrane. *J. Am. Chem. Soc.* **1982**, *104*, 4502–4503. (b) Ternansky, R. J.; Balogh, D. W.; Paquette, L. A. Dodecahedrane. *J. Am. Chem. Soc.* **1982**, *104*, 4503–4504.
- (14) (a) Prelog, V.; Seiwerth, R. New method for the preparation of adamantane. *Chem. Ber.* **1941**, *74*, 1769–1772. (b) Stetter, H.; Bänder, O.-E.; Neumann, W. Compounds with urotropine structure. VIII. New adamantane syntheses. *Chem. Ber.* **1956**, *89*, 1922–1926. (c) Fort, R.; Schleyer, P. v. R. Adamantane: Consequences of the Diamondoid Structure. *Chem. Rev.* **1964**, *64*, 277–300.
- (15) (a) Kroto, H. W.; Heath, J. R.; O’Brien, S. C.; Curl, R. F.; Smalley, R. E. C<sub>60</sub>: Buckminsterfullerene. *Nature* **1985**, *318*, 162–163. (b) Krätschmer, W.; Lamb, L. D.; Fostiropoulos, K.; Huffman, D. R. Solid C<sub>60</sub>: a new form of carbon. *Nature* **1990**, *347*, 354–358. (c) Curl, R. F.; Smalley, R. E. Fullerenes. *Sci. Am.* **1991**, *265* (4), 54–63. (d) *Recent Advances in the Chemistry and Physics of Fullerene and Related Materials*; Kadish, K. M., Ruoff, R. S., Eds.; The Electrochemical Society; Pennington, NJ, 1994; Vol. 1. (e) Lamparth, I.; Herzog, A.; Hirsch, A. Synthesis of [60]fullerene derivatives with an octahedral addition pattern. *Tetrahedron* **1996**, *52*, 5065–5075.

- (16) Leininger, S.; Fan, J.; Schmitz, M.; Stang, P. J. Archimedean solids: Transition metal mediated rational self-assembly of supramolecular-truncated tetrahedra. *Proc. Natl. Acad. Sci. U.S.A.* **2000**, *97*, 1380–1384.
- (17) Schweiger, M.; Yamamoto, T.; Stang, P. J.; Bläser, D.; Boese, R. Unpublished results.
- (18) *INSIGHT II 97.0*: Molecular Simulations, San Diego, CA, 1998.
- (19) Olenyuk, B.; Whiteford, J. A.; Fechtenkötter, A.; Stang, P. J. Self-assembly of nanoscale cuboctahedra by coordination chemistry. *Nature* **1999**, *398*, 796–799.
- (20) (a) Stejskal, E. O.; Tanner, J. E. Spin Diffusion Measurements: Spin-Echoes in the Presence of a Time-Dependent Field Gradient. *J. Chem. Phys.* **1965**, *42*, 288–292. (b) Haner, R. L.; Schleich, T. Measurement of Translational Motion by Pulse-Gradient Spin-Echo Nuclear Magnetic Resonance. *Methods Enzymol.* **1989**, *176*, 418–446.
- (21) (a) Beissel, T.; Powers, R. E.; Raymond, K. N. Coordination number incommensurate cluster formation. Part 1. Symmetry-based metal complex cluster formation. *Angew. Chem., Int. Ed. Engl.* **1996**, *35*, 1084–1086. (b) Beissel, T.; Powers, R. E.; Parac, T. N.; Raymond, K. N. Dynamic Isomerization of a Supramolecular Tetrahedral  $M_4L_6$  Cluster<sup>1</sup>. *J. Am. Chem. Soc.* **1999**, *121*, 4200–4206. (c) Caulder, D. L.; Powers, R. E.; Parac, T. N.; Raymond, K. N. The Self-Assembly of a Pre-designed Tetrahedral  $M_4L_6$  Supramolecular Cluster. *Angew. Chem., Int. Ed.* **1998**, *37*, 1840–1843. (d) Parac, T. N.; Caulder, D. L.; Raymond, K. N. Selective Encapsulation of Aqueous Cationic Guests into a Supramolecular Tetrahedral  $[M_4L_6]^{12-}$  Anionic Host<sup>1</sup>. *J. Am. Chem. Soc.* **1998**, *120*, 8003–8004.
- (22) (a) Kusukawa, T.; Fujita, M. Encapsulation of Large, Neutral Molecules in a Self-Assembled Nanocage Incorporating Six Palladium(II) Ions. *Angew. Chem., Int. Ed.* **1998**, *37*, 3142–3144. (b) Kusukawa, T.; Fujita, M. “Ship-in-a-Bottle” Formation of Stable Hydrophobic Dimers of *cis*-Azobenzene and -Stilbene Derivatives in a Self-Assembled Coordination Nanocage. *J. Am. Chem. Soc.* **1999**, *121*, 1397–1398. (c) Ibukuro, F.; Kusukawa, T.; Fujita, M. A Thermally Switchable Molecular Lock. Guest-Templated Synthesis of a Kinetically Stable Nanosized Cage. *J. Am. Chem. Soc.* **1998**, *120*, 8561–8562. (d) Ito, H.; Kusukawa, T.; Fujita, M. Wacker oxidation in an aqueous phase through the reverse phase-transfer catalysis of a self-assembled nanocage. *Chem. Lett.* **2000**, 598–599. (e) Fujita, M.; Oguro, D.; Miyazawa, M.; Oka, H.; Yamaguchi, K.; Ogura, K. Self-assembly of ten molecules into nanometre-sized organic host frameworks. *Nature* **1995**, *378*, 469–471. (f) Yoshizawa, M.; Kusukawa, T.; Fujita, M.; Yamaguchi, K. Ship-in-a-Bottle Synthesis of Otherwise Labile Cyclic Trimers of Siloxanes in a Self-Assembled Coordination Cage. *J. Am. Chem. Soc.* **2000**, *122*, 6311–6312.
- (23) Olenyuk, B.; Levin, M. D.; Whiteford, J. A.; Shield, J. E.; Stang, P. J. Self-Assembly of Nanoscopic Dodecahedra from 50 Pre-designed Components. *J. Am. Chem. Soc.* **1999**, *121*, 10434–10435.
- (24) Fujita, M.; Yu, S.-Y.; Kusukawa, T.; Funaki, H.; Ogura, K.; Yamaguchi, K. Self-Assembly of Nanometer-Sized Macrotricyclic Complexes from Ten Small Component Molecules. *Angew. Chem., Int. Ed.* **1998**, *37*, 2082–2085.
- (25) Radhakrishnan, U.; Schweiger, M.; Stang, P. J. Metal-Directed Formation of Three-Dimensional  $M_3L_2$  Trigonal-Bipyramidal Cages. *Org. Lett.* **2001**, *3*, 3141–3143.
- (26) (a) Saalfrank, R. W.; Stark, A.; Peters, K.; von Schnering, H. G. The First “Adamantoid” Alkaline Earth Metal Chelate Complex: Synthesis, Structure, and Reactivity. *Angew. Chem., Int. Ed.* **1988**, *27*, 851–853. (b) Saalfrank, R. W.; Burak, R.; Breit, A.; Stalke, D.; Herbst-Irmer, R.; Daub, J.; Porsch, M.; Bill, E.; Müther, M.; Trautwein, A. X. Mixed-Valence, Tetranuclear Iron Chelate Complexes as Endoreceptors: Charge Compensation Through Inclusion of Cations. *Angew. Chem., Int. Ed. Engl.* **1994**, *33*, 1621–1623. (c) Saalfrank, R. W.; Hörner, B.; Stalke, D.; Salbeck, J. The First Neutral Adamantanoid Iron(III) Chelate Complex: Spontaneous Formation, Structure, and Electrochemistry. *Angew. Chem., Int. Ed. Engl.* **1993**, *32*, 1179–1182. (d) Saalfrank, R. W.; Stark, A.; Bremer, M.; Hummel, H.-U. Formation of Tetranuclear Chelate-(4-) Ions of Divalent Metals (Mn, Co, Ni) with Idealized  $T$  Symmetry by Spontaneous Self-assembly. *Angew. Chem., Int. Ed. Engl.* **1990**, *29*, 311–314.
- (27) Schweiger, M.; Seidel, S. R.; Schmitz, M.; Stang, P. J. Rational Design of Chiral Nanoscale Adamantanoids. *Org. Lett.* **2000**, *2*, 1255–1257.
- (28) *Chem3D Pro 3.5.2*: CambridgeSoft Corp., Cambridge, MA, 1996.
- (29) (a) Fujita, M.; Nagao, S.; Ogura, K. Guest-Induced Organization of a Three-Dimensional Palladium(II) Cagelike Complex. A Prototype for “Induced-Fit” Molecular Recognition. *J. Am. Chem. Soc.* **1995**, *117*, 1649–1650. (b) Hiraoka, S.; Fujita, M. Guest-Selected Formation of Pd(II)-Linked Cages from a Prototypical Dynamic Library. *J. Am. Chem. Soc.* **1999**, *121*, 10239–10240. (c) Hiraoka, S.; Kubota, Y.; Fujita, M. Self- and hetero-recognition in the guest-controlled assembly of Pd(II)-linked cages from two different ligands. *Chem. Commun.* **2000**, 1509–1510. (d) Ikeda, A.; Udzu, H.; Zhong, Z.; Shinkai, S.; Sakamoto, S.; Yamaguchi, K. A Self-Assembled Homooxalix[3]arene-based Dimeric Capsule Constructed by a Pd<sup>II</sup>-Pyridine Interaction Which Shows a Novel Chiral Twisting Motion in Response to Guest Inclusion. *J. Am. Chem. Soc.* **2001**, *123*, 3872–3877. (e) Ikeda, A.; Yoshimura, M.; Udzu, H.; Fukuhara, C.; Shinkai, S. Inclusion of [60]Fullerene in a Homooxalix[3]arene-Based Dimeric Capsule Cross-Linked by a Pd<sup>II</sup>-Pyridine Interaction. *J. Am. Chem. Soc.* **1999**, *121*, 4296–4297. (f) Liu, H.-K.; Sun, W.-Y.; Ma, D.-J.; Yu, K.-B.; Tang, W.-X. The first X-ray structurally characterized  $M_3L_2$  cage-like complex with tetrahedral metal centres and its encapsulation of a neutral guest molecule. *Chem. Commun.* **2000**, 591–592.
- (30) Kuehl, C. J.; Yamamoto, T.; Seidel, S. R.; Stang, P. J. Self-Assembly of Molecular Prisms via an Organometallic “Clip”. *Org. Lett.* **2002**, *4*, 913–915.
- (31) Kuehl, C. J.; Kryschenko, Y. K.; Radhakrishnan, U.; Seidel, S. R.; Huang, S. D.; Stang, P. J. Self-assembly of nanoscopic coordination cages of  $D_{3h}$  symmetry. *Proc. Natl. Acad. Sci. U.S.A.* **2002**, *99*, 4932–4936.
- (32) (a) Kuehl, C. J.; Huang, S. D.; Stang, P. J. Self-Assembly with Postmodification: Kinetically Stabilized Metalla-Supramolecular Rectangles. *J. Am. Chem. Soc.* **2001**, *123*, 9634–9641. (b) Kuehl, C. J.; Mayne, C. L.; Arif, A. M.; Stang, P. J. Coordination-Driven Assembly of Molecular Rectangles via an Organometallic “Clip”. *Org. Lett.* **2000**, *2*, 3727–3729.

AR010142D